Thermal Expansion of Chemically Modified Mullite

by

Jie Tu

Thesis submitted to the Faculty of the

Virginia Polytechnic Institute and State University

in partial fulfillment of the requirements for the degree of

Master of Science

in

Materials Engineering

APPROVED:

Jesse J. Brown, Jr., Chairman

Robert E. Swanson

Paul H. Ribbe

May, 1988

Blacksburg, Virginia

Thermal Expansion of Chemically Modified Mullite

by

Jie Tu

Jesse J. Brown, Jr., Chairman

Materials Engineering

(ABSTRACT)

Solid-state reaction and sol-gel processing techniques were used extensively to form chemically-modified mullite solid solutions in an effort to lower their thermal expansion coefficients. TiO_2, B_2O_3, $CrPO_4$, P_2O_5, Ga_2O_3, Cr_2O_3, and WO_3 and the half-breed SiO_2 compounds $AlPO_4$, BPO_4, $GaPO_4$, $BAsO_4$, $AlAsO_4$, $GaAsO_4$, and GeO_2 were chosen as the modifiers.

The results indicate that, apart from TiO_2, none of the substitutions made in mullite significantly change the thermal expansion properties. The solubility of 3 wt% TiO_2 in mullite reduces the coefficient of thermal expansion by about 10%. That corresponds to a reduction in Al_2O_3/SiO_2 molar ratio (< 1.5) compared to stoichiometric mullite ($3Al_2O_3 \cdot 2SiO_2$). The formation of TiO_2-modified mullite depends on processing condition and heat treatment.

The possible mechanism of lowering the CTE of mullite by the addition of TiO_2 is discussed in terms of the bond strength. The axial expansion of a Ga_2O_3-modified mullite was measured up to 1200°C to show that the expansion is increased along the c-axis compared with that of the stoichiometric mullite.

Acknowledgements

I would like to give special thanks to Dr. J. J. Brown whose advice, guidance, and support have been invaluable. His understanding and patience made this M.S., especially the end of it, certainly less stressful and finally possible. I would like to extend special appreciation to Dr. R. E. Swanson who contributed valuable guidance throughout this research. My gratitude is also extended to Dr. P. H. Ribbe and Prof. F. A. Hummel for providing valuable advice and support concerning this work.

I would also like to express sincere appreciation to:

for her aid in the preparation of research reports.

and for their help concerning SEM lab and electron microprobe analysis, respectively.

for her encouragement and assistance during this period of study.

Colleagues and

for their assistance, advice, and friendship.

Last, but most of all, I wish to thank my parents without whose sacrifices all this would not be possible.

Table of Contents

List of Illustrations

List of Tables

Introduction

The need for ceramic materials with low thermal expansion chemically stable for use as components of advanced heat engines was recognized recently. Engine components such as regenerator disks and bulkheads in the hot flow path operate under thermal cyclic conditions which require low thermal expansion and high thermal shock resistance and must maintain integrity up to 1200°C in order for heat engines to have high combustion efficiency. The analytical equations for thermal shock resistance are based on the following equation:

$$\Delta T_f \simeq \frac{\sigma_f(1-\mu)}{E\alpha},$$

where ΔT_f is the temperature difference sufficient to cause fracture, σ_f is the stress required to fracture, μ is the Poisson's ratio, E is the modulus of elasticity, and α is the linear thermal expansion coefficient. The equation represents the simplest case, because it only considers that an elastic material fractures when the surface stress reaches a particular level. It assumes that the thermal conductivity of most ceramic materials is rather low. The equation also applies directly when the quench is so rapid that surface

temperatures reach their final value before the average temperature of the bulk specimen changes. The following is a more general equation:

$$\Delta T_f = \frac{\sigma_f(1-\mu)}{E\alpha} F(k,h,d),$$

in which F denotes a function of k, h, and d, where k is the thermal conductivity, h is the surface heat-transfer coefficient, and d is the sample dimension. Only k is positively correlated to the ΔT_f.

Since ceramic materials with higher σ_f tend to have higher E, changes in one of these two factors tend to be cancelled by the other, thus leaving α as the main variable influencing thermal shock resistance. Implicit in an interest in low expansion ceramics is a need for resistance to thermal shock, among other engineering considerations.

Some nonoxide systems such as silicon nitride (Si_3N_4) and silicon carbide (SiC), which show moderate low expansion and high mechanical strength, have been developed for use as engine components such as turbine rotors, vanes, and combustors. However, they principally have two disadvantages: oxidation damage and limitation of usage at high temperatures.

Two ceramic systems, $MgO\text{-}Al_2O_3\text{-}SiO_2$ (near compostion of the compound cordierite) and $Li_2O\text{-}Al_2O_3\text{-}SiO_2$ (near compostion of the compound spodumene), have been evaluated extensively for use in fabricating these low expansion ceramic components. However, ceramic materials based on either cordierite or spodumene have relatively low mechanical strength at high temperatures.

Mullite has high mechanical strength, relatively low thermal conductivity, good chemical stability, good thermal shock resistance, and moderate lattice anisotropy.[1] The present study focuses on chemically modified mullite. The deviation from stoichiometry by solid solution formation with other ions is utilized to attempt to reduce the thermal expansion.

Related Literature

Mullite exists as a solid solution with a typical composition of $Al_2^{VI}(Al^{IV}_{2+2x}, Si^{IV}_{2-2x})O_{10-x}\square_x$ [2,3] where IV and VI represent the oxygen coordination number of the cation and x is the number of oxygen vacancies per unit cell ($0.2 < x < 0.6$). The substitution of Al^{3+} for Si^{4+} in the tetrahedral chain of alternating $[SiO_4]$ and $[AlO_4]$ units introduces oxygen vancancies: $2Al^{3+} + \square = 2Si^{4+} + O^{2-}$. The crystal structure of mullite shown in Figure 1[4,5] is a projection on the (001) plane. Two unit cells show the effect of removing one Oc atom but do not exhibit the true symmetry resulting from statistical absence of Oc and rearrangement of cations. The oxygen atom, Oc, is shared by two tetrahedra and is the only oxygen atom that is not shared with an octahedron.[4,5] The range of x values is both temperature-dependent[4] and processing-dependent.[5] The Al_2O_3-SiO_2 phase diagram in the region of mullite solid solution at temperatures above 1600°C is shown in Figure 2.[4] The solid solution boundaries of mullite change with increasing temperature and join at 1890°C at a composition of 77.2 wt% Al_2O_3. The incongruent melting point of mullite is 1890°C with a peritectic between 76.5 and 77.0 wt%.[4] The remarkable range of compositions is due to the existence of a superstructure[6] which allows a variation in stoichiometry by changing the

repeat distance of the ordering periodicity. Conventionally, the compositions of $3Al_2O_3 \cdot 2SiO_2$ ($x=0.25$) and $2Al_2O_3 \cdot SiO_2$ ($x=0.4$) are considered to be the stoichiometric mullites.

Since the mullite structure has relatively wide channels running parallel to the c-axis,[7] it is suitable for incorporation of other ions. Gelsdorf *et al.*[8] found the following solubility limits; 8 wt% Fe_2O_3, 9 wt% Cr_2O_3, 2.5 wt% TiO_2, 1.5 wt% BeO, and 6 wt% V_2O_5 when quenching in air from 1200°C - 1700°C. They also reported a possible complete solid solution series existing between $3Al_2O_3 \cdot 2SiO_2$ and $9Al_2O_3 \cdot 2B_2O_3$, however the data given in the paper were not convincing. Phase equilibria of the system Al_2O_3-SiO_2-TiO_2 was studied by Agamawi *et al.*[33] and Galakhov.[34] However, their study did not indicate the formation of a limited solid solution series between mullite and TiO_2. Murthy and Hummel[9] also investigated additions of TiO_2, Fe_2O_3, and Cr_2O_3 to mullite (3:2). Their results agree with those of Gelsdorf except that Murthy and Hummel found that the solubility of Fe_2O_3 at 1300°C in mullite was 10 to 12 wt%. McKee and Wirkus[10] confirmed Murthy's result on the amounts of Fe_2O_3 and TiO_2 soluble in mullite. Swiecki *et al.*[11] later reexamined the maximum amount of Cr_2O_3 that could be introduced into mullite and found it to be 10 wt% at 1500°C. Bandin *et al.*[12] investigated solid solution of TiO_2 in mullite by X-ray dispersive energy techniques and found it to be 2.9 wt% at 1600°C. Recently, the temperature-dependent Fe_2O_3 solubility in mullite was determined by Schueidar[13] and found to be 10.5 wt% at 1300°C and 2.5 wt% at 1670°C by using electron microprobe analyses. The measurement of the lattice parameters of Fe-substituted mullite was carried out by Cardile *et al.*[14]. Both works suggested that Fe^{3+} substituted for Al^{3+} in octahedral sites. Except for Schueidar,[13] most studies have focused on cation-substituted 3:2 mullite.

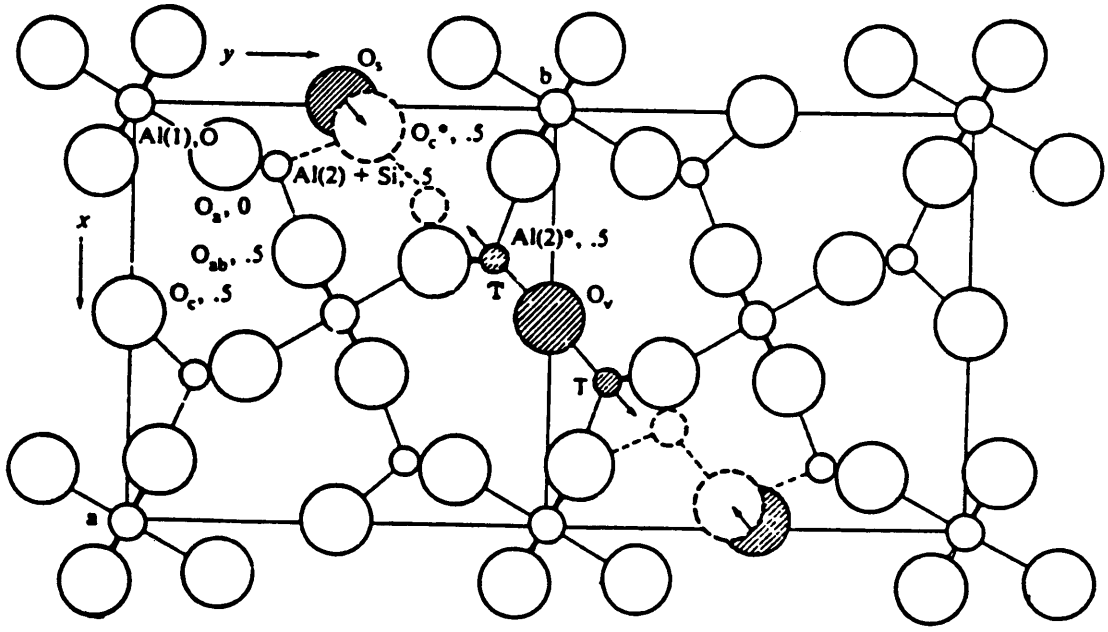

Figure 1. Project on (001) of the mullite structure; two unit cells show the effect of removing one Oc atom. Ov = oxygen removed, T = untenable tetrahedral site, O_s = oxygen shifted.[45]

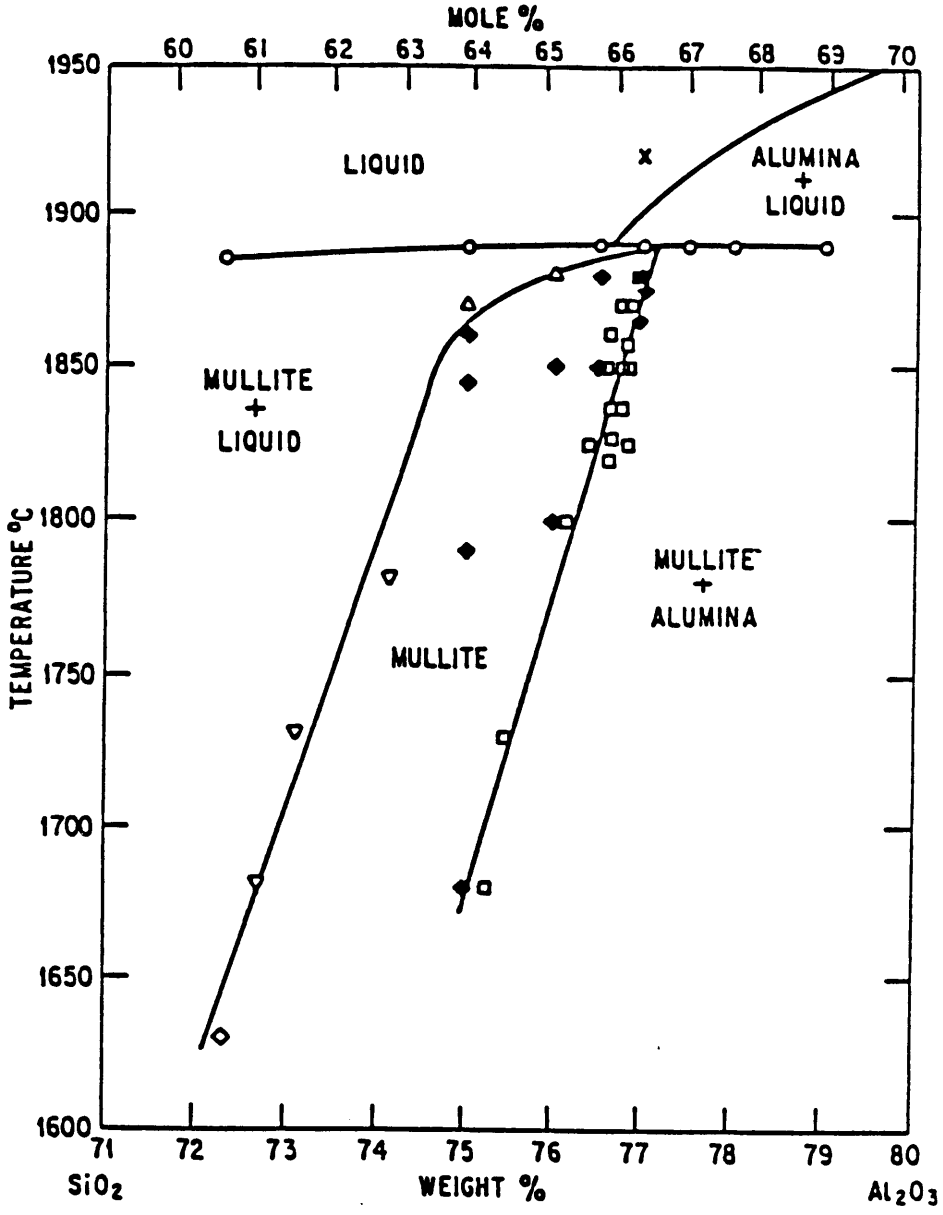

Figure 2. The Al_2O_3-SiO_2 phase diagram in the mullite(ss) region at $T \geq 1600°C$ showing solid solution boundaries to be temperature-dependent.[4]

The thermal expansion of solids is well understood from the fundamental perspective of the anharmonic effects on the equilibrium bond distances.[50] It results from the fact that although atoms vibrate about an average position, the distances between average positions change with temperature.[39] The greater the bonding forces (the deeper and more narrow the potential energy trough), the lower the change in position. For this reason the covalent and some of the ionic solids have the lowest coefficients of expansion. If the potential energy curve were symmetric, there would be no net change in interatomic separation, and, consequently, no thermal expansion.[49]

The thermal expansions of individual structural coordination polyhedra have been considered and completely explained by Hazen *et al.*[39] However, except for special situations, crystal structure effects on the thermal expansion are not as well characterized. Several of those special situations are the common fixed structures, including NaCl, CsCl, fluorite, rutile, and corundum, all of which exhibit bulk thermal expansions that are similar to the thermal expansions of their cation-anion bonds. Taylor[51] interpreted the thermal expansion behaviour of the framework silicates as due mainly to the effect of the rotation of the tetrahedra towards the fully-expanded state modified by anisotropic thermal motion of the framework oxygens and distortion of the tetrahedra from a regular form. Megaw[47] tried to express the thermal expansion of a crystal structure empirically as a linear combination of the expansions of its constituent parts. She also found that the expansion of a three-dimensional framework is the sum of a bond-length expansion and a tilting effect. Bond-length expansion coefficients are roughly equal to the inverse square of the Pauling valence (v).

The thermal expansion of sillimanite which is both structurally and compositionally similar to mullite was fully studied by Winter *et al.*[51] They found that all the Al

octahedra exhibit considerable expansions with increasing temperature, in contrast, Al- or Si-tetrahedra remain relatively constant in size and shape as temperature is increased. They concluded that the shared octahedral edges in sillimanite result in evenly distributed coefficients of unit-cell expansion.

Mullite (3:2) has a linear aggregate coefficient of thermal expansion (hereafter, CTE) of 5.3×10^{-6}/°C from 0°C to 1000°C.[1] The axial expansions of single crystal mullite (3:2) are $\alpha_a \simeq \alpha_b = 4.5\times10^{-6}$/°C and $\alpha_c = 5.7\times10^{-6}$/°C from room temperature to 1000°C.[1] Few investigations had been conducted to reduce the thermal expansion of single-phase mullite solid solution. Fenstermacher and Hummel[15] reported that 3:2 mullite has a slightly lower CTE value than 2:1 mullite. Lepold *et al.*[16] showed that the CTE of a mullite-glass composite decreased with increasing Al_2O_3/SiO_2 ratio. Kim[17] reported that the solid solution of all compositions lying on or near the join $9Al_2O_3{\cdot}2B_2O_3$ - $3Al_2O_3{\cdot}2SiO_2$ had CTEs of approximately 4.2×10^{-6}/°C. An aluminum titanate - mullite composite having low thermal expansion was developed by Morishima *et al.*[18] They reported that the thermal shock resistance tended to increase with increasing aluminum titanate content. Composites with less aluminum titanate have lower thermal shock resistance but have higher strength.

Experimental Procedure

I. Crystal Chemical Considerations

1. Ionic size

It is well known that two elements can usually substitute for one another if their ionic radii differ by less than 15%. If the radii of two ions differ by more than 15%, little or no substitution occurs. It is, therefore, essential that the radius of a selected cation be close to either the radius of Al^{3+} or Si^{4+} in order to form solid solution with mullite. Table 1 lists the radii[43] of all cations used in this study.

2. Electrical neutrality

Five types of substitution can exist in chemically modified mullite:

$$X^{4+} \text{-----} > Si^{4+}$$

$$4Y^{3+} \text{-----} > 3Si^{4+} + \square$$

$$Y^{3+} \text{-----} > Al^{3+}$$

$$3X^{4+} + \square \text{-----} > 4Al^{3+}$$

$$Y^{3+} + Z^{5+} \text{-----} > 2Si^{4+}$$

Where X, Y, and Z stand for cations having valence 4, 3, and 5, respectively.

Mullite itself has a defect structure characterized by the oxygen vacancies. By introducing or eliminating the vacancies and by having different sized foreign ions introduced into the structure, polyhedra distortion within the unit cell will vary in order to minimize the free energy of mixing. The larger the difference in the valence state between the substituting ion and Al^{3+} or Si^{4+}, the less likely solid solution will form.

3. Temperature and stoichiometry-dependent solubility

Al-rich (molar ratio of Al_2O_3/SiO_2 > 1.5) mullite forms if the firing temperature is greater than 1580°C. [4,32] Higher temperatures increase the degree of disorder of the Al/Si in the tetrahedral sites. Moreover, it is known that Al ions prefer IV coordination to VI coordination at high temperatures.[7] As a consequence, mullite formed at high temperatures display extensive ionic substitutions that would not be possible at lower temperatures. Furthermore, because of the distinct nonstoichiometric nature of mullite solid

solution, the incorporation of foreign ions into its structure depends on the heat treatment and chemical nature of the modifying cation.

4. Bond strength

A new bond strength parameter, $p = s/r$, was recently defined.[35] The r is the row number of the main group cations in the periodic table and s is the well-known Pauling bond strength, $s = v/CN$, where v is the valence state of cation and CN refers to the coordination number of a cation. The cation-oxygen bond in which the cation having a high electron static valence and low coordination expands upon heating less than the same bond having a low v and high CN. That is because the total electrostatic energy associated with a particular cation is distributed among fewer bonds when the CN is small. It is reasonable to expect that a polyhedron with strong bonds expands less than one with weak bonds. Table 1 lists some basic parameters[43] of selected cations for substitution in mullite.

II. Experimental Procedure

The compounds TiO_2, B_2O_3, $AlPO_4$, BPO_4, $CrPO_4$, $GaPO_4$, $BAsO_4$, $AlAsO_4$, $GaAsO_4$, P_2O_5, Ga_2O_3, GeO_2, Cr_2O_3, and WO_3 were chosen as the modifiers. These oxide compounds contain the cations which basically satisfy the crystal chemical requirements stated previously (see section I), with the exception of WO_3. In particular, GeO_2 and XYO_4 (except for $CrPO_4$) compounds are isostructural with certain silica

Table 1. Some basic parameters of selected cations.[43]

Cation	Valence (ν)	Coordination Number(CN)	Radius(Å)	Pauling Bond Strength(s)	Bond Strength(p)
Al	3	4	0.39	0.75	0.375
	3	6	0.535	0.5	0.25
Si	4	4	0.26	1	0.5
B	3	4	0.11	0.75	0.75
Cr	3	6	0.615	0.5	--
Ga	3	4	0.47	0.75	0.25
	3	6	0.62	0.5	0.167
Ge	4	4	0.39	1	0.333
	4	6	0.53	0.667	0.222
Ti	4	4	0.42	1	--
	4	6	0.605	0.667	--
P	5	4	0.17	1.25	0.625
As	5	4	0.335	1.25	0.417
W	6	6	0.6	1	--

polymorphs. [19-24] They have the three-dimensional network of corner-sharing [GeO_4], [PO_4], and [AsO_4] tetrahedra. Starting materials and heat treatments used to synthesize the compounds are listed in Table 2. Synthesis of those compounds was necessary because the volatility of both P_2O_5 and As_2O_5 are high, whereas their $X^{3+}Y^{5+}O_4$ compounds are much more stable on heating. All compositions were prepared by mixing the desired oxide powders under acetone. The oxide powders were heat-treated in alumina crucibles with lids following the firing schedules shown in Table 2.

Subsequent to each firing, the samples were removed from the furnace and thoroughly mixed using a mortar and pestle. Phases in the reacted samples were identified by XRD following each firing to assure that the desired product had been successfully synthesized.

A general processing technique was used to synthesize and fabricate the bars of chemically modified mullite by solid-state reaction as outlined in Figure 3. The sol-gel process involving hydrolysis of metal alkoxides [25-31] was also used to synthesize chemically modified mullite in an effort to obtain improved reaction due to the ultra-fine particle sizes, high homogeneity, and narrow particle-size distribution. This improves the diffusion in grain boundaries, lowers the sintering temperature, and possibly increases the solubility of selected cations in mullite. The starting materials were $Si(OC_2H_5)_4$, $Al[(CH_3)_2CHO]_3$, $Al[C_2H_5CH(CH_3)O]_3$, $Ti[OCH(CH_3)_2]_4$, $B(CH_3O)_3$, and $P(O)(CH_3O)_3$, and the procedure is outlined in Figure 4.

XRD phase identification was made on the sintered specimens using Cu$K\alpha$ radiation. The diffraction patterns were measured in a 2θ range from 15° to 70° with a scanning rate of 1° 2θ/min. and compared with ASTM powder data files. Unit cell parameters of four Ti-modified mullites were determined using the multiple linear regression method.

Table 2. Solid-state synthesis of the half-breed SiO_2 compounds [1].

Compound	Starting materials	Heat treatment (^{0}C/hr)[2]
$AlPO_4$	$Al(OH)_3 nH_2O$+1.01$(NH_4)_2HPO_4$	400/4 +800/10+1100/72[3]
BPO_4	H_3BO_3 +1.01$(NH_4)_2HPO_4$	400/4 +800/10+1050/72
$CrPO_4$	Cr_2O_3 +2.02$(NH_4)_2HPO_4$	400/2 +600/10+1080/48[4]
$GaPO_4$	Ga_2O_3 +2.02$(NH_4)_2HPO_4$	400/2 +600/10+1080/48
$BAsO_4$	$2H_3BO_3$ +1.01As_2O_3	100/2 +200/16+400/8+600/8+700/8
$AlAsO_4$	Al_2O_3 +1.01As_2O_3	200/16+400/8 +600/8+700/8+900/12
$GaAsO_4$	Ga_2O_3 +1.01As_2O_3	200/16+400/8 +600/8+700/8+900/12

[1] $CrPO_4$ is not isostructural with silica.
[2] Powders were taken out of furnace and reground after each heating step.
[3] Trace amount of $Al(PO_3)_3$ was detected.
[4] Trace amount of Cr_2O_3 was detected.

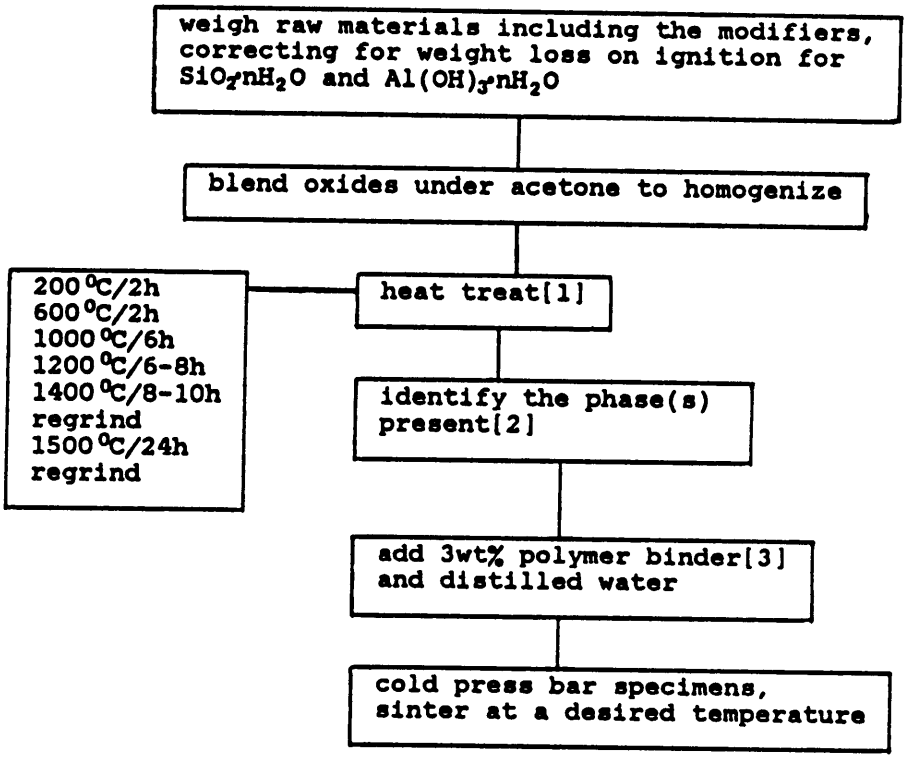

[1] Some reactants were sealed in a Pt-tube to prevent the loss of volatile material.
[2] XRD was used to identify the heat treated powders expected to contain mullite as a major phase before pressing them into a bar. A shrinkage in volume of a bar occurs if a bar is pressed directly from raw materals.
[3] Methocel 20-122 Cellulose Ether is manufactured by Dow Chemicals.

Figure 3. Flow chart for the production of solid-state synthesized, chemically-modified mullite.

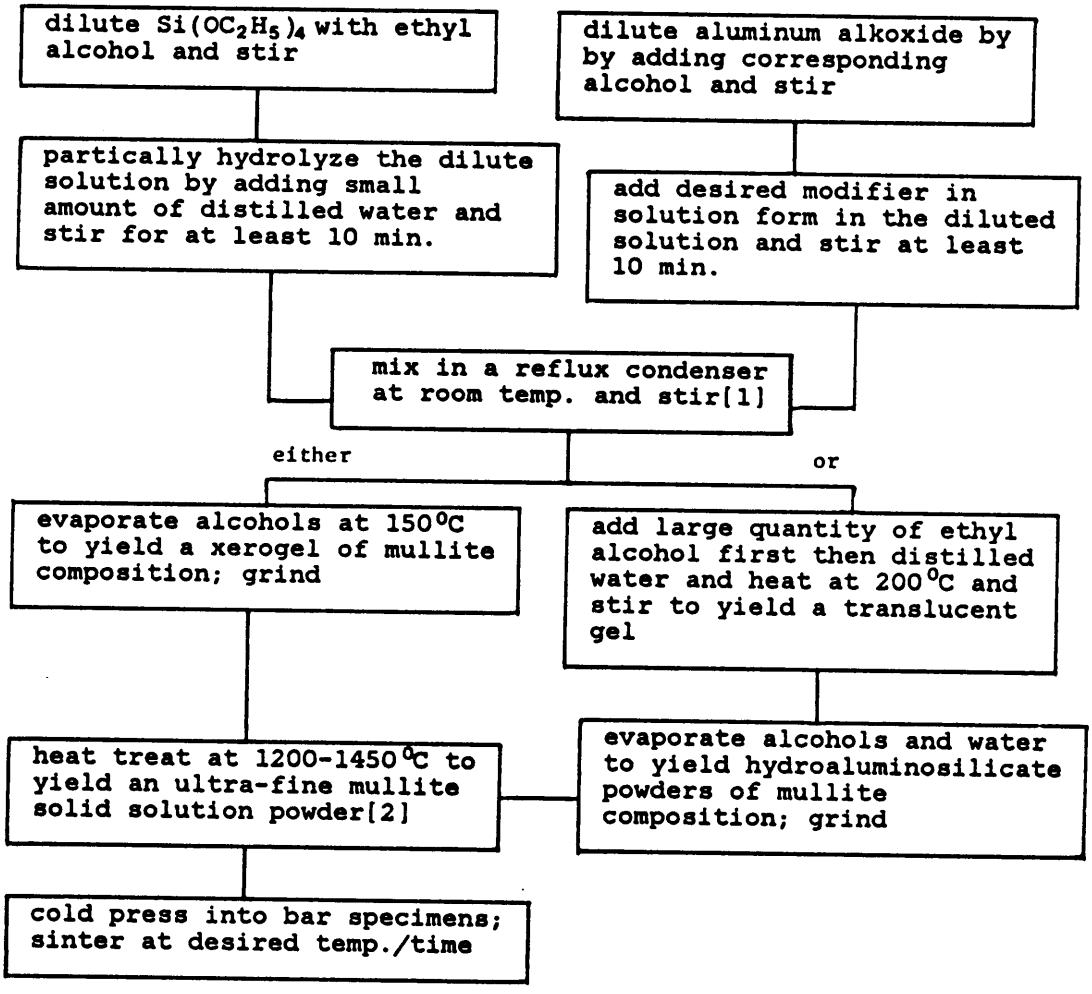

[1] The pH value of the solutions is usually maintained at 7.
[2] Powders are examined by XRD.

Figure 4. Flow chart for the production of sol-gel synthesized, chemically-modified mullite.

Fluorite (CaF_2) powder was used as the internal standard to correct the 2θ errors. High temperature XRD was used to determine the axial thermal expansion of a Ga-modified mullite using Pt powder as the internal standard.

All specimens were examined under the polarizing microscope to semiquantitatively determine the presence of different phases after sintering. It was also used to detect the presence of a glassy phase.

In order to determine the linear aggregate CTE of the samples, bar specimens 100 by 10 by 10 mm or 25 by 6 mm were pressed in a steel mold at 60 and 20 MPa, respectively. After the specimens were sintered at the desired temperature, the CTEs for the former were measured by means of a fused-silica dilatometer or an automated differential dilatometer using single crystal of sapphire to calibrate and alumina as a reference.

Results and Discussion

I. Sample Preparation

All samples were prepared by either solid-state reaction or sol-gel decomposition followed by high temperature reaction. The procedure used for each preparation is denoted in the various tables.

In the sol-gel synthesis the effect of different pH values of the solution containing mullite precursor on the microscopic feature of the powders was studied. During the sol-gel processing of the TiO_2-modified mullite, the solution was divided into three portions having pH 7 before being placed in a reflux condenser (see Figure 4). In two of the portions, the pH value was altered to 2 and 12 by adding HNO_3 and NH_4OH solutions, respectively. The solution of the portion with pH 2 appeared to be clear. The other two appeared to be somewhat milky. After stirring 24 hours at room temperature and drying at 200°C, the long-needle-like (1 to 15 mm) amorphous hydroaluminosilicates having mullite composition formed from the portion with pH 2. The other two portions

yielded ultra-fine equiaxed powders. This result indicated that under acidic condition (pH < 7) the polymerization occurred in the mullite precursor. The polymerization may be the formation of ...-Si-Al-Si-Al-Si-... chains.[46] The polymerization of the precursor later affects the size distribution of the particles after heat treatment. The powders from the three portions were fired at 1450°C for 24 hours to yield mullite. They were then examined by SEM to show that the portion with pH 2 after firing gave large (10-50 μm) aggregated particles. The two portions with pH 7 and 12 gave very small aggregated particles (1-5 μm), the latter yielded particles with the most uniform sizes. Therefore, it is recommended that a basic condition be used in sol-gel processing to obtain mullite with fine particle size and uniform size distribution.

Initially samples of TiO_2-modified mullite were heated at different temperatures in an effort to determine the optimum sintering/reaction range. XRD data showed that the samples sintered at 1500°C — 1600°C produced the least amount of Al_2TiO_5 and had the highest degree of mullite formation. Therefore, this temperature range was used throughout the remainder of this study.

These initial results also indicated that Al_2TiO_5 can coexist with TiO_2-modified mullite from 1450°C to 1600°C. When the temperature exceeds 1600°C, Al_2TiO_5 decomposes into Al_2O_3 plus rutile. This suggests that the composition of mullite changes above 1600°C to a more aluminum-rich mullite.

The electron microprobe was used to examine the distribution of Al_2TiO_5 and/or TiO_2 in the mullite solid solution after sintering at 1550°C. The X-ray mapping demonstrated that very fine Al_2TiO_5 and/or rutile crystals were dispersed inhomogeneously in the grains of mullite as well as in the grain boundaries.

Minor amounts of a glassy phase were found by polarized microscopy after the initial sintering at 1600°C. Because of this, the samples were resintered at a lower temperature (1400°C) in order to recrystallize the liquid phase. There are two possible reasons for the liquid formation. First, compositions with $1.5 \leq Al_2O_3/SiO_2 \leq 2.0$ are likely to form Al_2TiO_5. This reaction consumes Al_2O_3 and results in excess free SiO_2, which is glass forming. Lower temperature recrystallization gives Si a chance to diffuse into Al_2TiO_5 and forms a solid solution, which has been confirmed by other workers.[37] This is probably the reason free α-cristobalite was not observed after sintering. Secondly, according to the study of Aksay and Pask,[38] a metastable region of mullite plus liquid may form at 1700°C or lower, if the conditions are right, even if the initial formulation is 3:2, the stoichiometry composition of mullite.

II. TiO_2—Mullite Solid Solutions

The sample numbers, compositions, heat treatments, phase analyses, and coefficient of thermal expansion (CTE) values investigated are shown in Table 3 and 4. The samples listed in Table 3 were prepared by solid-state reactions and those in Table 4 by sol-gel decomposition.

These results show that insofar as final equilibrium phase assemblages are concerned, both preparation techniques yielded the same results. When the TiO_2 content was 3 wt% or less, mullite solid solutions formed; above 3 wt% TiO_2, Al_2TiO_5 formed as a second phase. This indicates that the solid solubility limit of TiO_2 is about 3 wt%. The variation of the unit cell dimensions over the solid solution region as determined by

Table 3. TiO_2 in mullite-based compositions by solid-state reaction.

Sample No.	Composition (wt%) Al_2O_3	SiO_2	TiO_2	A/S	Sintering (°C/h)	Phase(s) present	CTE(°C×10⁶) R.T.-1000°C
J-009	71.08	27.92	1.00	1.5	1600/6+1200/8	M[1]	4.8
J-010	70.36	27.64	2.00	1.5	1600/8+1200/8	M	4.9
J-011	69.64	27.36	3.00	1.5	1600/12+1200/19	M	4.7
J-012	68.92	27.08	4.00	1.5	1600/12+1200/19	M	5.0
J-013	68.21	26.79	5.00	1.5	1600/6+1400/38	M+R[2]	5.4
J-014	67.49	26.51	6.00	1.5	1600/6+1400/38	M+R	5.6
J-015[3]	67.85	26.65	5.00	1.5	1600/6+1400/38	M+R	5.3
J-016[4]	66.76	26.23	6.00	1.5	1600/6+1400/38	M+R	5.6
J-005	67.30	26.49	6.21	1.5	1600/8+1200/11	M+R	5.6
J-006	66.62	23.13	10.25	1.7	1600/8+1200/11	M+AT[5]	5.2
J-007	62.73	24.60	12.67	1.5	1600/8+1200/11	M+AT	3.5
J-008	62.15	21.55	16.30	1.7	1600/8+1200/11	M+AT	3.0
J-017	60.09	23.61	16.30	1.5	1600/12+1400/38	M+AT	3.2
J-018	64.65	19.05	16.30	2.0	1600/12+1400/38	M+AT	3.9
J-019	60.19	20.81	19.00	1.7	1600/12+1400/38	M+AT	2.5
J-020	57.96	20.04	22.00	1.7	1600/12+1400/38	M+AT	2.3
J-035	54.07	15.93	30.00	2.0	1100/4+1500/56	M+AT	2.0
J-036	47.32	12.68	40.00	2.2	1100/4+1500/56	M+AT+R	N.A.[6]

1. Mullite(ss) as a major phase
2. rutile
3. 0.5 wt% MgO added
4. 1.01 wt% MgO added
5. aluminum titanate(ss)
6. not available

Table 4. TiO_2-modified mullite synthesized by sol-gel processing.

Sample No.	Composition	A/S	Sintering (°C/h)	Phase(s) present	CTE(°C×10⁶) R.T.-1000°C
J-082	$Al_6Ti_{0.1}Si_{1.9}O_{13}$	1.58	1500/72	M	5.0
J-083	$Al_6Ti_{0.2}Si_{1.8}O_{13}$	1.67	1500/72	M	5.1
J-084	$Al_6Ti_{0.3}Si_{1.7}O_{13}$	1.76	1500/72	M + AT(tr)	N.A.
J-0901	$Al_{5.6}Ti_{0.3}\square_{0.1}Si_2O_{13}$	1.40	1350/72	M + R(mi)	N.A.
J-0902	$Al_{5.6}Ti_{0.3}\square_{0.1}Si_2O_{13}$	1.40	1450/72	M + AT(tr)	N.A.
J-0903	$Al_{5.6}Ti_{0.3}\square_{0.1}Si_2O_{13}$	1.40	1500/72	M + AT(tr)	N.A.
J-0904	$Al_{5.6}Ti_{0.3}\square_{0.1}Si_2O_{13}$	1.40	1550/72	M + AT(tr)	4.8
J-0905	$Al_{5.6}Ti_{0.3}\square_{0.1}Si_2O_{13}$	1.40	1600/72	M + AT(tr) + R(tr)	N.A.
J-0906	$Al_{5.6}Ti_{0.3}\square_{0.1}Si_2O_{13}$	1.40	1650/20	M + R(tr)	N.A.
J-0907	$Al_{5.6}Ti_{0.3}\square_{0.1}Si_2O_{13}$	1.40	melted	M + R(tr)	N.A.
J-091	$Al_{5.73}Ti_{0.19}\square_{0.07}Si_2O_{13}$	1.44	1550/72	M	4.6
J-093	$Al_{5.76}Ti_{0.18}\square_{0.06}Si_2O_{13}$	1.44	1550/72	M	5.0
J-094	$Al_{5.68}Ti_{0.24}\square_{0.08}Si_2O_{13}$	1.42	1550/72	M + AT(tr)	5.0

M = mullite(ss)
AT = Al_2TiO_5 (aluminum titanate)
R = rutile
N.A. = not available
tr = trace
mi = minor amount

multiple linear regression are shown in Table 5. The general trend is that the lattice constants a and b show a slight increase and that no significant change occurs along the c-axis. It is reasonable to speculate that the large Ti^{4+} occupying the lattice sites in place of Al^{3+} increases the x and y dimensions. The c-axial direction is the direction of alternating [AlO_4] and [SiO_4] chains and appears to be more adaptable to the size difference of the cation in the structure because the Si-O-Al bond angles are rather flexible. Generally when the TiO_2 content was between 4-6 wt% and the Al_2O_3/SiO_2 molar ratio was about 1.5, rutile also appeared.

As TiO_2 is added to mullite in solid solution, the thermal expansion coefficient was found to decrease slightly from 5.2×10^{-6}/°C to about 4.7×10^{-6}/°C at the solid solubility limit (Figure 5). Above 3 wt% TiO_2 when Al_2TiO_5 appears as a second phase, the CTE decreases significantly (Figure 6) due to the low CTE of pure Al_2TiO_5 ($< 1\times10^{-6}$/°C[1]). It should be noted that Al_2TiO_5 is extremely anisotropic ($\alpha_a \simeq \alpha_b = -2.6\times10^{-6}$/°C and $\alpha_c = 11.5\times10^{-6}$/°C).[1] Although mixtures of Al_2TiO_5 and mullite solid solution yield very low expansion coefficients, they will exhibit poor mechanical properties because of the anisotropic expansion of Al_2TiO_5.

Several samples containing 5-6 wt% TiO_2 were prepared to determine whether a small amount of MgO could promote more extensive TiO_2 solubility. It was observed that the addition of MgO had little or no effect on thermal expansion (Figure 7) of TiO_2-modified mullite, neither did MgO increase the solubility of TiO_2 in mullite.

Table 5. Unit cell dimensions of TiO_2-modified mullite over the solid solution region at room temperature.

Sample	a_o (Å)	b_o (Å)	c_o (Å)	V (Å^3)
J-009	7.539	7.684	2.883	167.01
J-010	7.551	7.690	2.893	167.99
J-011	7.549	7.692	2.888	167.70
J-012	7.555	7.699	2.890	168.10
3:2 mullite*	7.548	7.691	2.886	167.54

* Referenced from Ribbe[7]

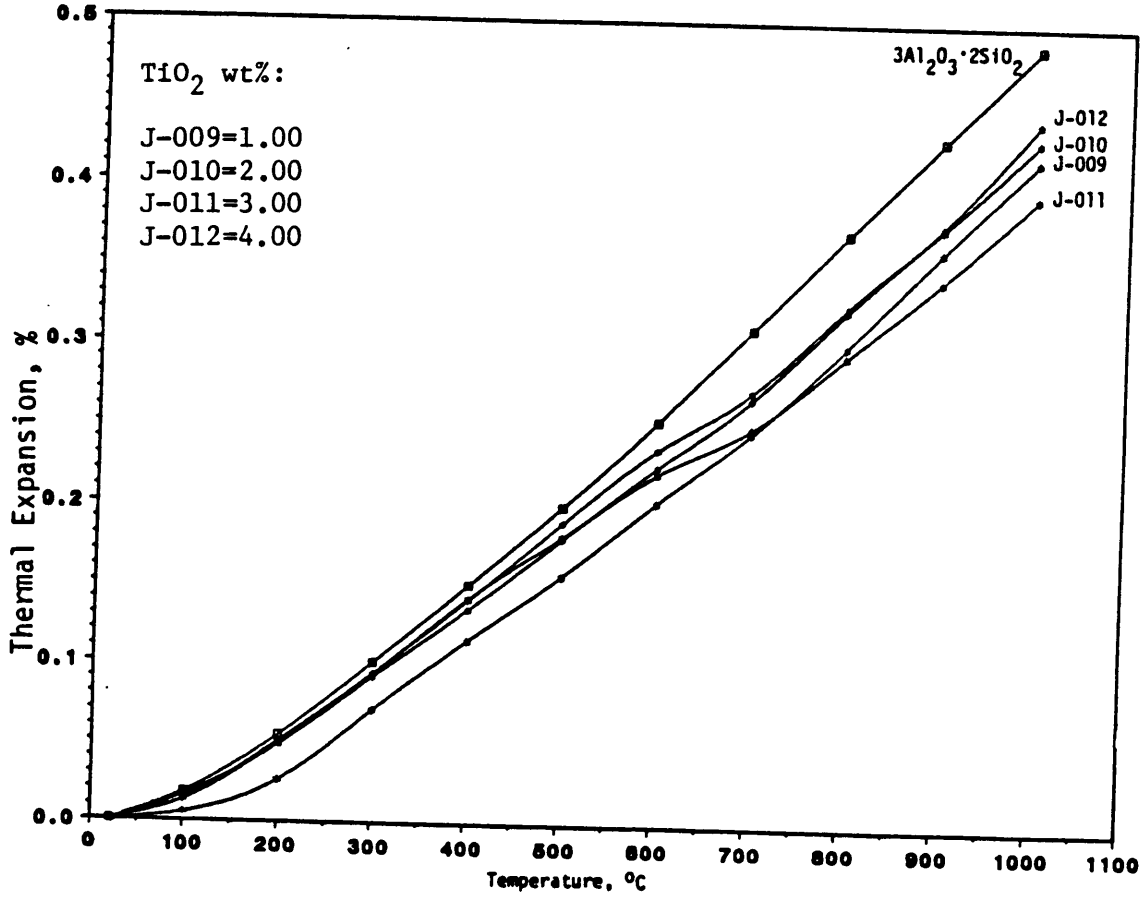

Figure 5. Thermal expansion of TiO_2-modified mullite solid solutions.

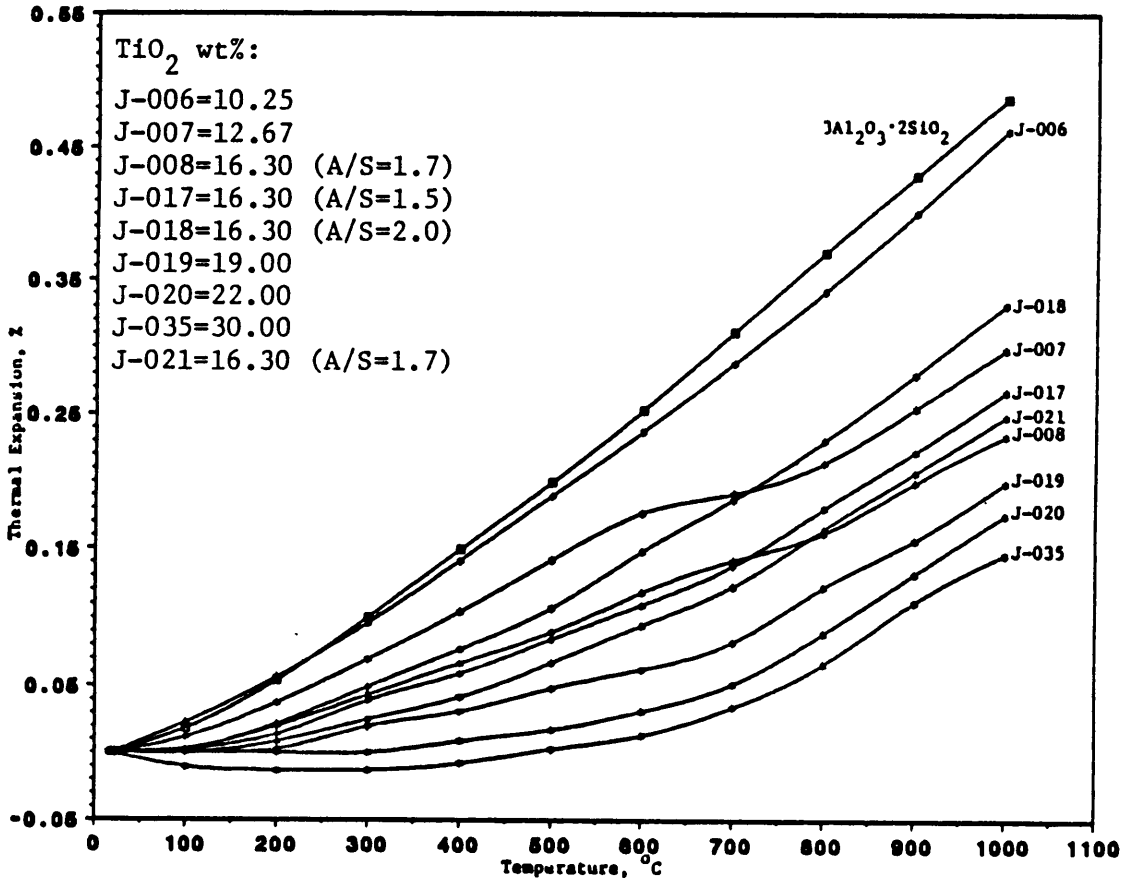

Figure 6. Thermal expansion of mullite-based bodies containing Al_2TiO_5.

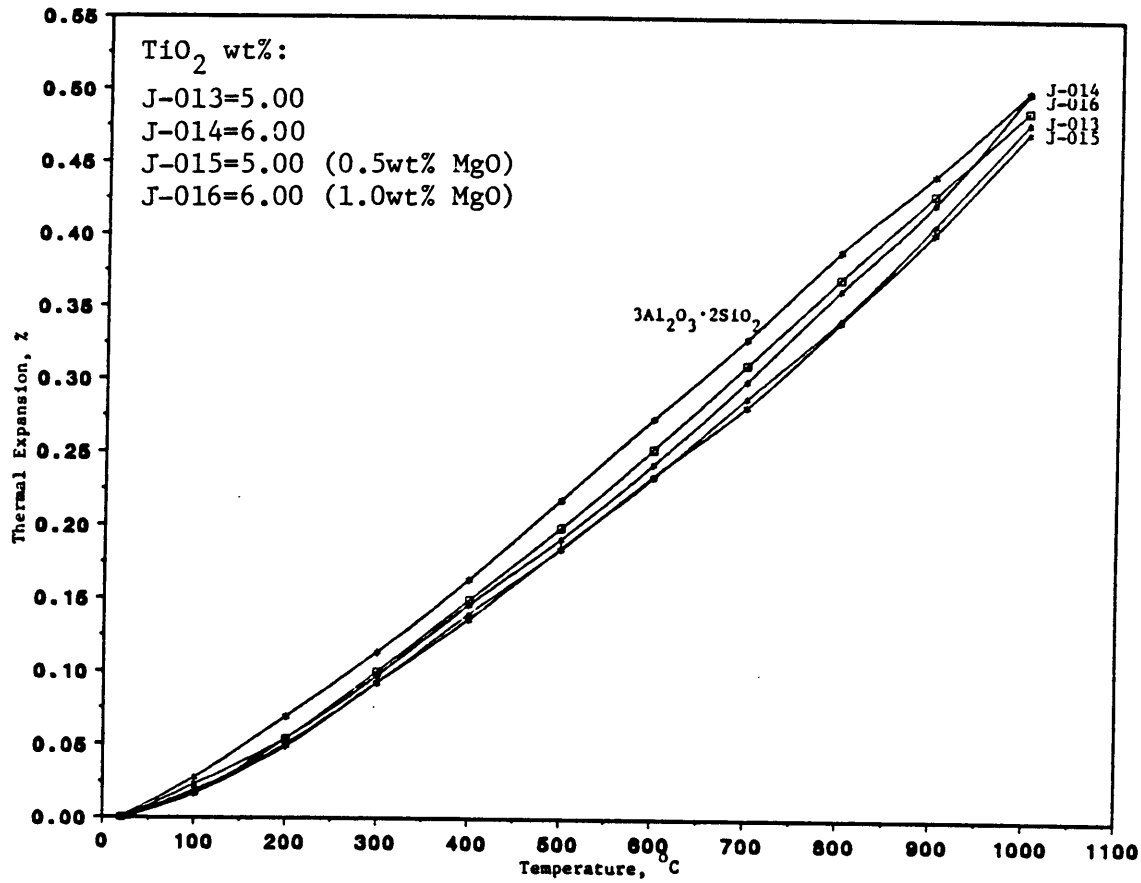

Figure 7. Thermal expansion of TiO_2 modified mullite solid solutions with/without MgO.

III. TiO_2—B_2O_3—Mullite Solid Solution

In an effort to reduce the CTE of TiO_2-modified mullite further, B_2O_3 was added. Based on the data given in Table 1, the B^{3+}—O^{2-} bond has a bond strength twice that of the Al^{3+}—O^{2-} bond. A series of B_2O_3-TiO_2-modified mullite compositions was prepared by sol-gel processing. The compositions, heat treatments, phases and CTE results are shown in Table 6. As can be seen, B_2O_3 has little if any effect on the thermal expansion of TiO_2-modified mullite.

IV. $AlPO_4$—BPO_4—Mullite Solid Solutions

Since $AlPO_4$ and BPO_4 are isostructural with SiO_2 and the ionic radii of P^{5+} and B^{3+} (see Table 1) are close to those of Si^{4+} and Al^{3+}, and since a charge-balanced substitution exists (see Experimental Procedure), limited solubility of both compounds in mullite can be expected. Moreover, P^{5+}—O^{2-} and B^{3+}—O^{2-} bonds have higher bond strength than Si^{4+}—O^{2-} or Al^{3+}—O^{2-} bond and may lower the CTE of mullite. The compositions listed in Table 7 were prepared and the phases present after reaction were identified. The most notable result was the absence of any significant formation of solid solution. Numerous preparation procedures were used including (a) mixing of $AlPO_4$ and BPO_4 with mullite followed by high temperature reaction; (b) mixing of ingredients such as H_3BO_3 and $(NH_4)_2HPO_4$ followed by high temperature reaction; (c) mixing of $AlPO_4$ and BPO_4 with mullite in a sealed Pt-tube which after reaction was quenched in ice water in an attempt to maintain high temperature equilibrium;[41] and (d) sol-gel for-

Table 6. B_2O_3-TiO_2-modified mullite system.

Sample No.	Composition	A/S	Sintering (°C/h)	Phase(s) Present	CTE(°C×10⁶) R.T.-1000°C
J-054*	$Al_{5.2}B_{0.8}Si_2O_{13}$	1.3	1500/24	M + g(tr)	5.0
J-055*	$Al_{4.8}B_{1.2}Si_2O_{13}$	1.2	1500/24	M + g(tr)	5.1
J-072	$Al_{5.2}B_{0.8}Si_2O_{13}$	1.3	1550/72	M	5.2
J-086	$Al_{5.1}B_{0.9}Si_{1.7}Ti_{0.3}O_{13}$	1.5	1550/80	M + AT(tr)	N.A.
J-089	$Al_{4.94}B_{0.80}Ti_{0.2}\square_{0.07}Si_2O_{13}$	1.24	1550/80	M	4.9
J-092	$Al_{5.14}B_{0.6}Ti_{0.2}\square_{0.07}Si_2O_{13}$	1.29	1550/72	M	5.1

* synthesized by solid-state reaction
g = glassy phase
tr = trace
M = mullite(ss)
A/S = Al_2O_3/SiO_2 molar ratio

mation followed by high temperature reaction. None of the preparations showed significant mullite solid solution. Compositions containing less than 3 wt% $AlPO_4$ and BPO_4 were sintered for 216 hours (three 3-day periods) at 1500°C. Multiphase assemblage were still observed by XRD. It must be acknowledged that even after these long heat treatments it is very possible that equilibrium was still not achieved.

In the composition containing both BPO_4 and $AlPO_4$, the change of d-spacing for $AlPO_4$ confirmed the formation of $(Al,B)PO_4$ solid solution. The overall solubility of $(Al,B)PO_4$ in mullite seems to be very low (< 3 wt%).

The thermal expansion curves for selected compositions are shown in Figure 8. As can be seen, there is little difference in the curves when compared with that of mullite except variations in the 200—600°C range which is due to the presence of $(Al,B)PO_4$ which has a polymorphic inversion in this range.

V. XYO_4—Mullite Solid Solutions

Table 8 lists the compositions prepared from adding half-breed derivatives (excluding $AlPO_4$ and BPO_4) to mullite. Except for $CrPO_4$, all compounds are isostructural with SiO_2. All compositions were prepared by solid-state reaction using synthesized XYO_4 compounds as well as the raw materials Cr_2O_3, $(NH_4)_2HPO_4$, H_3BO_3, Ga_2O_3, $Al(OH)_3 \cdot nH_2O$, and $SiO_2 \cdot nH_2O$. as starting materials. The three arsenates were synthesized first instead of using the raw oxides because As_2O_5 is very volatile and its

Table 7. $AlPO_4$-BPO_4-modified mullite system.

Sample No.	Composition (wt%) Al_2O_3	SiO_2	$AlPO_4$	BPO_4	A/S	Sintering (°C/h)	Phase(s) present	CTE(°C×10⁶) R.T.-1000°C
J-022[1]	66.77	26.23	7.00	--	1.5	1600/5+1500/72	M[5] + AP[6](t) + C[7](t)[9]	5.3
J-023[1]	63.18	24.82	12.00	--	1.5	1600/5+1500/72	M+AP(t)+C(t)	5.4
J-024[1]	59.59	23.41	17.00	--	1.5	1600/5+1500/72	M+AP(t)	--
J-026[1]	61.67	26.33	12.00	--	1.38	1600/5+1500/72	M+AP(t)	5.4
J-027[1]	66.87	26.13	--	7.00	1.5	1550/18	M+ABP[8](t)+C(t)	5.0
J-028[1]	63.28	24.72	--	12.00	1.5	1550/18	M+ABP(t)	5.5
J-029[2]	64.70	25.30	2.78	7.22	1.5	1550/18	M+ABP(t)+C(t)	--
J-030[2]	64.70	25.30	5.36	4.64	1.5	1550/18	M+ABP(t)+C(t)	--
J-031[2]	64.70	25.30	7.76	2.24	1.5	1550/18	M+ABP(t)+C(t)	--
J-032[3]	68.31	26.69	5.00	--	1.5	1500/12+1600/18	M+AP(t)+C(t)	--
J-033[3]	68.31	26.69	--	5.00	1.5	1500/12+1600/18	M+ABP(t)+C(t)	--
J-034[3]	64.70	25.30	5.00	5.00	1.5	1500/12+1600/18	M+ABP(t)+C(t)	--
J-036[2]	59.56	28.08	--	12.36	1.25	1500/27	M+ABP(t)	5.8
J-057[2]	58.46	27.56	13.98	--	1.25	1500/27	M+AP(t)	5.6
J-067[4]	68.40	26.87	--	4.73	1.5	1500/27	M+ABP(t)	--
J-068[4]	67.91	26.68	5.41	--	1.5	1500/12	M+AP(t)	--
J-075[2]	71.76	25.37	2.86	--	1.67	1500/216	M+AP(t)+C(t)	--
J-076[2]	72.04	25.47	--	2.49	1.67	1500/216	M+ABP(t)+C(t)	--

1. Synthesized $AlPO_4$ and BPO_4 were used as raw materials.
2. $(NH_4)_2HPO_4$ and H_3BO_3 were used as the sources of P_2O_5 and B_2O_3.
3. Sample was sintered in a sealed Pt-tube and quenched in ice water. Powders were reagent grade SiO_2, Al_2O_3, $AlPO_4$, and BPO_4.
4. Samples were prepared by sol-gel processing.
5. M = mullite(ss)
6. AP = $AlPO_4$
7. C = corundum
8. ABP = $(Al,B)PO_4$
9. t = trace amount

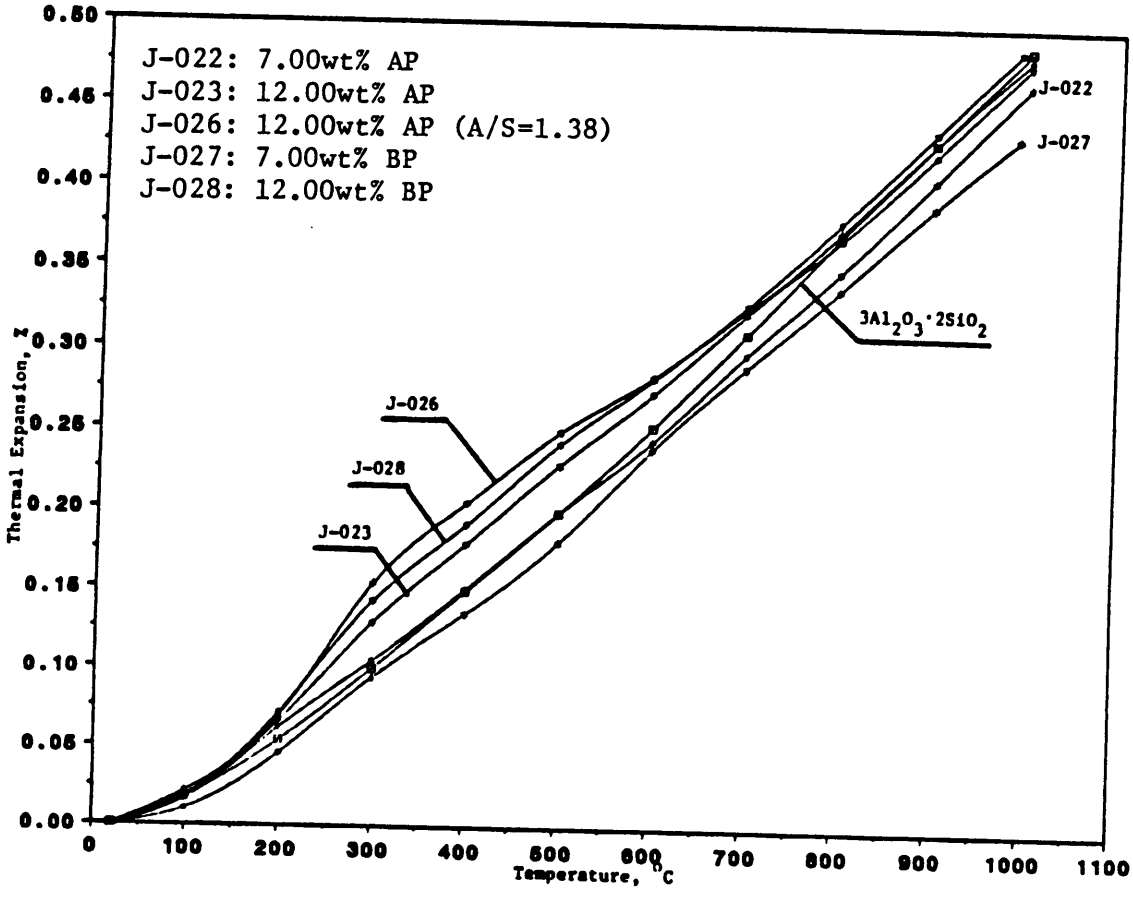

Figure 8. Thermal expansion of $AlPO_4$-BPO_4-mullite-based system.

melting point is below 500°C. Moreover, the arsenates have higher melting point than As_2O_5 and are relatively more stable at higher temperature.

Only $GaAsO_4$ showed the formation of significant mullite solid solution. Other compositions having higher Al_2O_3/SiO_2 values showed the formation of two or more phases. The formation of small amount of liquid phase in preparations containing $BAsO_4$, $AlAsO_4$, and $GaAsO_4$ was also observed. The CTE values of selected compositions were determined to be in the range 5.0 to 5.8×10^{-6}/°C. It appears that the CTE values obtained did not vary significantly from that of stoichiometric mullite.

VI. Single Oxides (P_2O_5, Ga_2O_3, GeO_2, B_2O_3, Cr_2O_3, and WO_3)—Mullite(ss)

The addition of various simple oxides having the general formula A_xO_y were reacted with mullite in an effort to form solid solution. The compositions, heat treatments, phase analyses, and CTEs are listed in Table 9. The results can be summarized as follows.

(1) P_2O_5 did not show significant solubility in mullite, even though P^{5+} ions can be readily incorporated into many other silicates in the $[SiO_4]$ positions. This phenomenon may be explained by the formation of the very stable $AlPO_4$ consuming most of the P_2O_5 before it has a chance to diffuse into the mullite structure. It may also be speculated that P^{5+} substituting for Si^{4+} introducing cation vacancies into mullite is crystallographically difficult.

Table 8. XYO_4 compound-modified mullite(ss).

Sample No.	Composition (wt%) Al_2O_3	SiO_2	XYO_4	A/S	Sintering (°C/h)	Phase(s) Present	CTE(°C×10⁶) R.T.-1000°C
J-052	68.20	26.80	5.00$GaPO_4$	1.5	1500/24	M[2] + C[3](t)[4]	5.8
J-053	68.20	26.80	5.00$CrPO_4$	1.5	1550/24	M + C(t)	5.6
J-058	62.63	27.34	10.03$CrPO_4$	1.35	1550/27	M + (Al,Cr)PO_4	5.6
J-059	61.88	27.01	11.11$GaPO_4$	1.35	1550/27	M + (Al,Ga)PO_4	5.0
J-060	65.54	27.59	6.87$BAsO_4$	1.4	1550/42	M + g[5](t)	5.3
J-061	65.06	27.38	7.56$AlAsO_4$	1.4	1550/42	M + g(t)	5.2
J-062	63.81	26.86	9.33$GaAsO_4$	1.4	1550/42	M + g(t)	5.0
J-063	60.10	26.23	13.66$GaAsO_4$	1.35	1550/30	M	5.1
J-077[1]	71.05	25.12	3.83$GaPO_4$	1.67	1500/216	M + (Al,Ga)PO_4(t) + C(t)	--
J-078[1]	71.35	25.23	3.43$CrPO_4$	1.67	1500/216	M + (Al,Cr)PO_4(t) + C(t)	--
J-079	71.30	25.21	3.49$BAsO_4$	1.67	1500/216	M + C(t)	--
J-080	71.03	25.11	3.85$AlAsO_4$	1.67	1500/216	M + C(t)	--
J-081	70.33	24.87	4.80$GaAsO_4$	1.67	1500/216	M + C(t)	--

1. Prepared by solid-state reaction with Ga_2O_3, Cr_2O_3 , and $(NH_4)_2HPO_4$ as raw materials
2. M = mullite(ss)
3. C = corundum
4. t = trace amount
5. g = glassy phase

Table 9. Simple oxide-modified mullite(ss).

Sample No.	Composition	A/S	Sintering (°C/h)	Phase(s) Present	CTE(°C×10⁶) R.T.-1000°C
J-039	$Al_6Si_{1.875}P_{0.1}\square_{0.025}O_{13}$	1.60	1550/24	M[3] + AP[4](t)[7]	--
J-040	$Al_6Si_{1.75}P_{0.2}\square_{0.05}O_{13}$	1.71	1550/24	M + AP(t) + C[5](t)	--
J-069[1]	$Al_{5.91}Si_{1.87}P_{0.158}\square_{0.0394}O_{13}$	1.58	1500/100	M + AP(t)	--
J-037	$Al_{5.4}Ga_{0.6}Si_2O_{13}$	1.35	1500/56	M	4.9
J-041	$Al_5Ga\ Si_2O_{13}$	1.25	1500/56	M + G[6](t)	4.8
J-042	$Al_{4.6}Ga_{1.4}Si_2O_{13}$	1.15	1500/56	M + G(t)	4.8
J-048	$Al_6Ge_2O_{13}$	--	1450/48	Ge-M	5.2
J-038	$Al_{5.4}Ga_{0.6}Si_{1.5}Ge_{0.5}O_{13}$	1.8	1500/56	M + C(t)	5.2
J-044	$Al_5GaSi_{1.5}Ge_{0.5}O_{13}$	1.67	1500/56	M + C(t)	5.1
J-045	$Al_{5.1}Ga_{0.6}Ti_{0.2}\square_{0.07}Si_2O_{13}$	1.28	1550/24	M + G(t)	4.9
J-047	$Al_{5.4}Ga_{0.3}Ti_{0.2}\square_{0.07}Si_2O_{13}$	1.35	1550/24	M	5.0
J-046	$Al_{5.1}Ga_{0.6}Ti_{0.2}\square_{0.07}Si_{1.75}Ge_{0.25}O_{13}$	1.46	1550/24	M	5.1
J-054	$Al_{5.2}B_{0.8}Si_2O_{13}$	1.3	1550/30	M	5.0
J-055	$Al_{4.8}B_{1.2}Si_2O_{13}$	1.2	1550/30	M	5.1
J-072[1]	$Al_{5.2}B_{0.8}Si_2O_{13}$	1.3	1550/100	M	5.2
J-049[2]	$Al_{5.48}Cr_{0.52}Si_2O_{13}$	1.37	1550/30 + 1600/24	M	4.7
J-050	$Al_{5.8}W_{0.1}\square_{0.1}Si_2O_{13}$	1.45	1550/24	M + W[8](t)	5.4
J-051	$Al_{5.6}W_{0.2}\square_{0.2}Si_2O_{13}$	1.4	1550/24	M + W(t)	5.5

1. Synthesized by sol-gel processing
2. Amount of Cr_2O_3 used corresponds to its solid solubility in mullite at 1600°C
3. M = mullite(ss)
4. AP = $AlPO_4$
5. C = corundum
6. G = α-Ga_2O_3
7. t = trace amount
8. W = WO_3

(2) Ga_2O_3 showed an extended solubility in mullite. The solid solution formation of Ga_2O_3 in mullite was investigated based on the following stoichiometry:

$$Al_{6-x}Ga_xSi_2O_{13}.$$

Ga_2O_3-mullite(ss), having the values of x from 0 to 2.2, were prepared by both solid-state reaction and sol-gel techniques. Values of x up to 1.8 in the compositions gave mullite solid solution. However, compositions in the solid solution range did not yield CTE values significantly different from that of stoichiometric mullite.

The axial expansion of specimen $(Al_5Ga)Si_2O_{13}$ was measured by high temperature XRD to determine whether Ga in mullite changes the expansion anisotropy. The axial expansions are characterized by three independent principal linear expansion coefficients, α_a, α_b, α_c. Figure 9 shows the variation of the lattice parameters as a function of temperature. Compared to those of 3:2 mullite (see Table 4), all three axial parameters of Ga_2O_3-modified mullite at room temperature are about 5 to 8% larger than stoichiometric mullite because of the larger ionic radius of Ga^{3+}. It was obsvered that all three axes have higher average CTE values at the low temperature region than at the high temperature region. The average values of α_a and α_b from room temperature to 1200°C are approximately equal to those of stoichiometric mullite; however, the c-axial expansion is significantly larger. The expansion anisotropy of mullite increases due to the addition of Ga_2O_3.[1] Such an increase in anisotropy during heating is not desireable because it causes grain-boundary microcracking. The addition of Ga_2O_3 with small amounts TiO_2 and GeO_2 to mullite was shown to have had practically no effect on thermal expansion of mullite(ss).

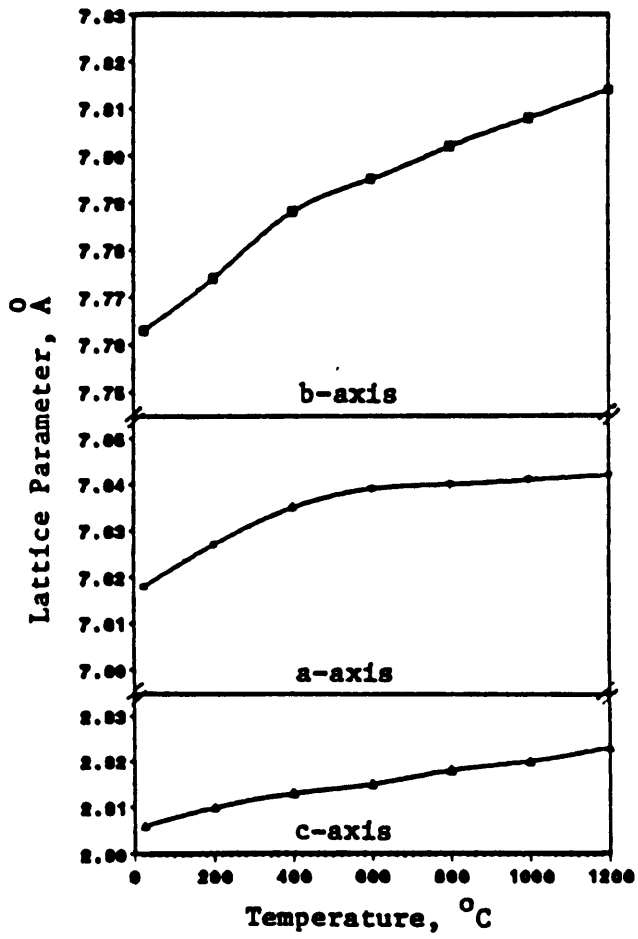

Figure 9. Axial expansion for Ga_2O_3-modified mullite solid solution.

(3) GeO_2 was found to form a complete solid solution series between $Al_6Si_2O_{13}$ — $Al_6Ge_2O_{13}$ with Ge^{4+} substituting for Si^{4+} in the tetrahedral sites. Based on the following stoichiometry, $Al_6(Si_{2-x}Ge_x)O_{13}$, specimens with x values up to 2 were investigated. The CTE values did not change significantly with the addition of GeO_2.

It was previously reported[42] that GeO_2 has only limited solid solubility in cordierite, and that GeO_2-modified cordierite has a lowered CTE from room temperature to 500°C even though the Ge-O bond is electrostatically weaker than the Si-O bond. Structurally, mullite does not have the large channels surrounded by the $[SiO_4]$ and $[AlO_4]$ rings that cordierite has. It is obvious that the differences in crystal structure between these two minerals play a decisive role in affecting the thermal expansion as well as affecting the ability of Ge^{4+} to substitute for Si^{4+}.

(4) B^{3+} substituting for Al^{3+} in the tetrahedral sites in mullite should increase the bond strength. However, the samples investigated did show significant solid solubility but did not show a significant change in CTE. Further, liquid phase formation was frequently observed even with low heating rates.

(5) $Al_{5.48}Cr_{0.52}Si_2O_{13}$ represents the maximum amount of Cr_2O_3 soluble[9] in mullite. The CTE value shows a slight decrease in comparsion with stoichiometric mullite. This solid solution series should be studied further.

(6) WO_3-modified mullite was prepared based on the following stoichiometry:

$$Al_{6-2x}W_x\square_xSi_2O_{13}.$$

WO_3 does not seem to be soluble in mullite which is probably due to the the large difference in their valence states.

VII. Crystal Chemical Observations

The mechanism of decreasing the CTE of mullite by the addition of TiO_2 may be explained by consideration of bond strengths and the variation of bond lengths and bond angles. Structurally Ti^{4+} can substitute into three available sites in mullite, namely $[AlO_6]$, $[AlO_4]$, and $[SiO_4]$. Crystal chemically, however, Ti^{4+} will most likely go into $[AlO_6]$ sites rather than $[AlO_4]$ sites, because radius ratio of Ti ions prefers 6-coordination.

The bond strengths(s) are shown by the data in Table 1. In an octahedral site, Ti^{4+} has a Pauling bond strength of 0.7 with O^{2-} which is one-third greater than Al^{3+} with O^{2-}. Thus $[TiO_6]$ octahedral site should expand less upon heating than $[AlO_6]$ after the substitution (also see Hazen and Finger).[39] In terms of the tetrahedral site, because the Si^{4+}—O^{2-} bond has a bond strength twice that of the Al^{3+}—O^{2-} bond, the $[SiO_4]$ would expand less than $[AlO_4]$ upon heating (Figure 10). This can be supported by the experimental result (Figure 11) which showed that a deficiency in Al is favored over a deficiency in Si in the stoichiometry in reducing the CTE of mullite: the compositions of $Al_{6-4y}Ti_{3y}\square_ySi_2O_{13}$ is favored over the compositions of $Al_6Si_{2-x}Ti_xO_{13}$, more precisely, in the range of $1.44 \leq Al_2O_3/SiO_2 \leq 1.67$ (see Table 3 and 4).

The variations of bond lengths and bond angles could not be fully verified because of the lack of high temperature crystallographic data. But it is known[47] that when polyhedra are linked by their corners, titling becomes possible. In mullite such titlings however are restricted by the edge-sharing $[AlO_6]$. Nevertheless, it has been well demonstrated[39] that the octahedral site expands more than the tetrahedral site upon

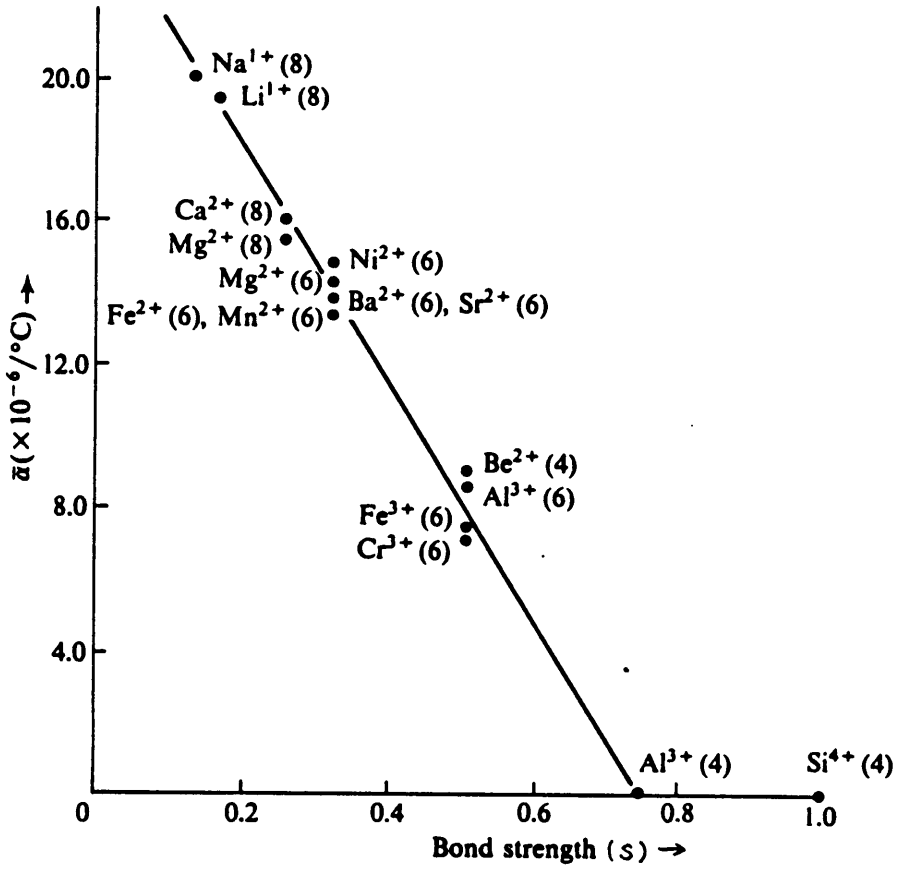

Figure 10. Variation of mean CTEs of various cation polyhedra with Pauling bond strength (s). Numbers in parentheses are CN.[48]

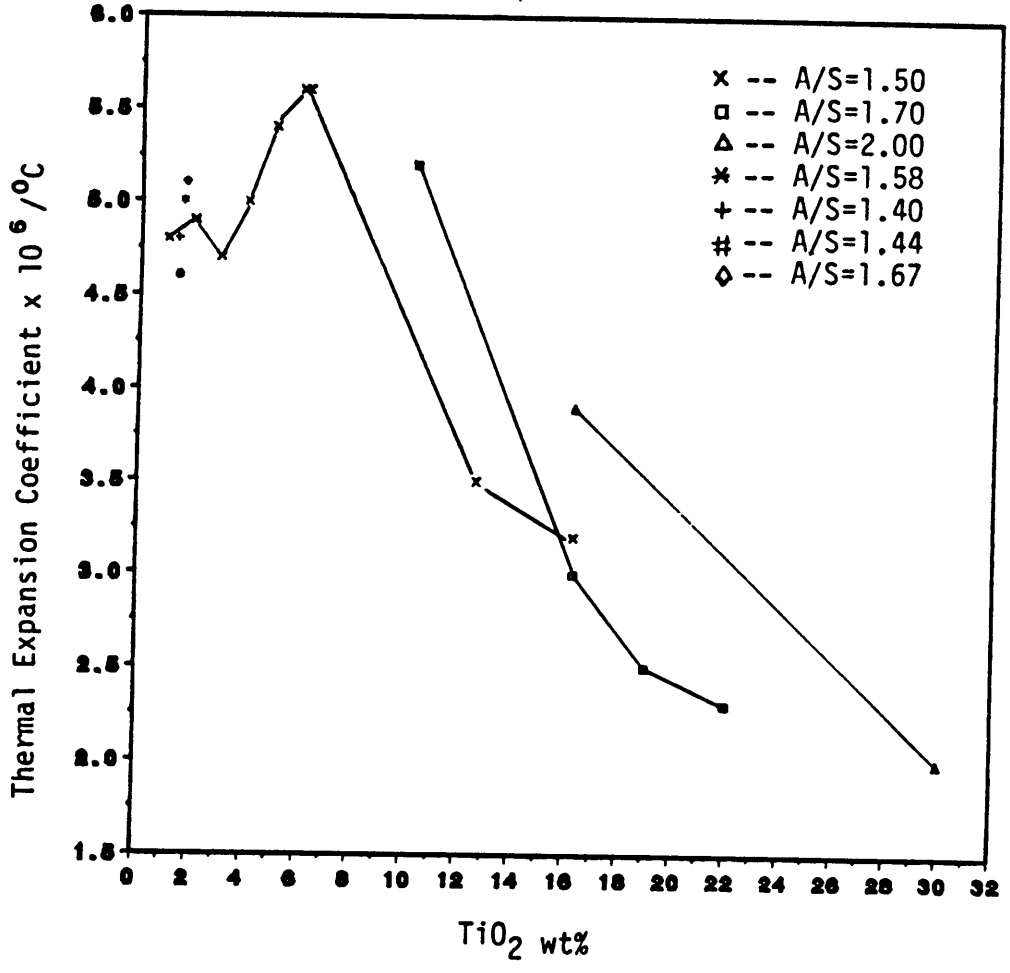

Figure 11. CTE in the TiO_2-mullite-based system with varying Al_2O_3/SiO_2 molar ratio.

heating in almost all types of crystal structures. The most influential fact of the expansion in mullite probably is the bond strength with anions of those cations in octahedral sites. The tetrahedral sites, on the other hand, because of their strong bonding, need only to vary the bond angles. It is therefore desired to replace Al^{3+} with other cations having higher charges ($v > 3$) and small ionic radius[39] (less than that of Al^{3+} in octahedral site) in order to increase the bond strength in the site. Hence, it is desired to achieve the solid solubility of that cation in mullite in order to have the maximum effect on thermal expansion.

The effect of having oxygen vacancies (oxygen deficiency) generated by Al^{3+} substituting for Si^{4+} and cation vacancies generated Ti^{4+} substituting for Al^{3+} on thermal expansion of defect mullite(ss) is not fully understood. However, calculation shows that 2:1 mullite has 4% oxygen positions vacant and 3:2 mullite has 2.5% oxygen positions vacant. Sample $Al_{5.73}Ti_{0.19}\square_{0.07}Si_2O_{13}$, having the CTE $4.6\times10^{-6}/°C$, gives an additional 1% of the Al^{3+} sites vacant. Numerically, the percentage is too small to be significant. But structurally, it may have played an important role in affecting the thermal expansion of the lattice.

Summary

1. Apart from TiO_2, none of the substitutions attempted in mullite changed the thermal expansion properties significantly.

2. Sol-gel processing appears to decrease the time required for mullite formation at high temperatures, but produces the same results (solubility and phase assemblage) as solid-state reaction.

3. The solubility of 3 wt% TiO_2 in mullite reduces the thermal expansion coefficient by about 10%. This corresponds to a reduction in the Al_2O_3/SiO_2 molar ratio compared to stoichiometric mullite.

4. Substitution of half-breed derivatives such as $AlPO_4$, BPO_4, *etc.* in mullite is very limited and the equilibrium condition is difficult to achieve. Single oxides (except for GeO_2 and Ga_2O_3) such as B_2O_3, P_2O_5, *etc.* show low solubilities in mullite.

References

1. W. D. Kingery, H. K. Bowen, and D. R. Uhlmann, Introduction to Ceramics, 2nd Edition, John Wiley & Sons, 1976.

2. W. E. Cameron, "Mullite: A Substituted Alumina," *Amer. Mineral.*, **62**, 747-55 (1977).

3. R. J. Angel and C. T. Prewitt, "Crystal Structure of Mullite: A Reexamination of the Average Structure," *Amer. Mineral.*, **71**, 1476-82 (1986).

4. Frederic J. Klug and Svante Prochazka, "Alumina-Silica Phase Diagram in the Mullite Region," *J. Am. Ceram. Soc.*, **70** [10] 750-9 (1987).

5. J. A. Pask, X. W. Zhang, and A. P. Tomsia, "Effect of Sol-Gel Mixing on Mullite Microstructure and Phase Equilibia in the α-Al_2O_3-SiO_2 System," *J. Am. Ceram. Soc.*, **70** [10] 704-7 (1987).

6. J. D. C. McConnell and V. Heine, "Incommensurate Structure and Stability of Mullite," *Phys. Rev. B: Condens. Matter*, **31** [9] 6140-2 (1985).

7. P. H. Ribbe, Orthosilicates, *Reviews in Mineralogy*, Vol.5, 189-214, 2nd Edition, Mineralogical Society of America, 1982.

8. V. G. Gelsdorf, H. Müller-Hesse, and H-E. Schwiete, "Einlagerungsversuche an Synthetischem Mullit und Substitutionsversuche mit Galliumoxyd und Germaniumdioxyd Teil II," *Archiv für das Eisenhüttenwesen*, **29** [8] 513-9 (1958).

9. M. K. Murthy and F. A. Hummel, "X-ray Study of the Solid Solution of TiO_2, Fe_2O_3, and Cr_2O_3 in Mullite ($3Al_2O_3 \cdot 2SiO_2$)," *J. Am. Ceram. Soc.*, **43** [5] 267-71 (1960).

10. T. D. McKee and C. D. Wirkus, "Mullitization of Alumino-Silicate Gels," *Amer. Ceram. Soc. Bull.*, **51** [7] 577-81 (1972).

11. Z. Swiecki, J. Chmielewski, and W. Zolnierczyk, "X-ray Analysis of Mullite with additions of Chromium (III)," *Szklo Ceram.*, **27** [7] 176-81 (1976).

12. C. Bandin, M. I. Osendi, and J. S. Moya, "Solid Solution of TiO_2 in Mullite," *J. Mater. Sci. Lett.*, **2** [5] 185-7 (1983).

13. H. Schneider, "Temperature-dependent Iron solubility in Mullite," *J. Am. Ceram. Soc.*, **70** [3] C-43-C-45 (1987).

14. C. M. Cardile, I. W. M. Brown, and K. J. D. Mackenzie, "Mossbauer Spectra and Lattice Parameters of Iron-Substituted Mullites," *J. Mater. Sci. Lett.*, **6** [3] 357-62 (1987).

15. J. E. Fenstermacher and F. A. Hummel, "High-Temperature Mechanical Properties of Ceramic Materials: IV, Sintered Mullite Bodies," *J. Am. Ceram. Soc.*, **44** [6] 185-7 (1961).

16. M. H. Leipold and J. D. Sibold, "Development of Low-Thermal Expansion Mullite Bodies," *J. Am. Ceram. Soc.*, **65** [9] C-147-C-149 (1982).

17. K. H. Kim, "Phase Equilibria in the System Li_2O- B_2O_3-Al_2O_3-SiO_2 and Some of its Subsidiary Systems," Ph.D. Thesis, the Pennsylvania State University (1961).

18. H. Morishima, Z. Kato, K. Uematsu, and K. Saito, "Development of Aluminum Titanate-Mullite Composite Having High Thermal Shock Resistance," *J. Am. Ceram. Soc.*, **69** [10] C-266-C-267 (1986).

19. F. A. Hummel, "Properties of Some Substances Isostructural with Silica," *J. Am. Ceram. Soc.*, **32** [10] 320-6 (1949).

20. M. J. Buerger, "The Stuffed Derivatives of the Silica Structures," *Amer. Mineral.*, **39** [7-8] 600-14 (1954).

21. E. C. Shafer and R. Roy, "Studies of Silica-Structure Phases: I, $GaPO_4$, $GaAsO_4$, and $GaSbO_4$," *J. Am. Ceram. Soc.*, **39** [10] 330-6 (1956).

22. J. F. Sarver, "Thermal-Expansion Data for Rutile-Type GeO_2," *J. Am. Ceram. Soc. Discussions & Notes*, **46** [4] 195-6 (1963).

23. A. Rulmont, P. Tarte, and J. M. Winand, "Vibrational Spectrum of Crystalline and Glassy $LiBGeO_4$: Structural Analogies with $BAsO_4$," *J. Mater. Sci. Lett.*, **6** 659-62 (1987).

24. J. P. Attfield, A. W. Sleight, and A. K. Cheetham, "Structure Determination of α-$CrPO_4$ from Powder Synchrotron X-Ray Data," *Nature*, **322** [14] 620-2 (1986).

25. K. S. Mazdiyasni and L. M. Brown, "Synthesis and Mechanical Properties of Stoichiometric Aluminum Silicate (Mullite)," *J. Am. Ceram. Soc.*, **55** [11] 548-52 (1972).

26. B. L. Metcalfe and J. H. Sant, "The Synthesis, Microstructure and Physical Properties of High Purity Mullite," *Trans. J. Brit. Ceram. Soc.*, **74** [31] 193-201 (1975).

27. T-I. Mah amd K. S. Mazdiyasni, "Mechanical Properties of Mullite," *J. Am. Ceram. Soc.*, **66** [10] 699-703 (1983).

28. D. W. Hoffman, R. Roy, and S. Komarneni, "Diphasic Xerogels, A New Class of Materials: Phases in the System Al_2O_3-SiO_2," *J. Am. Ceram. Soc.*, **67** [7] 468-71 (1984).

29. Q-M. Yuan, J-Q. Tan, J-Y. Shen, X-H. Zhu, and Z-F. Yang, "Processing and Microstructure of Mullite-Zirconia Composites Prepared from Sol-Gel Powders," *J. Am. Ceram. Soc.* **69** [3] 268-9 (1986).

30. B. E. Yoldas *et al.*, *Low Temperature Formation of Mullite*, U. S. Pat. Appl. U. S. 867,727 (Oct. 10, 1986).

31. K. Okada and N. Otsuka, "Characterization of the Spinel Phase from SiO_2-Al_2O_3 Xerogels and the Formation Process of Mullite," *J. Am. Ceram. Soc.*, **69** [9] 652-56 (1986).

32. S. Aramaki and R. Roy, "Revised Equilibrium Diagram for the System Al_2O_3-SiO_2," *J. Am. Ceram. Soc.*, **45** [5] 229-42 (1962).

33. Y. M. Agamawi and J. White, "System Al_2O_3-TiO_2-SiO_2," *Trans. Brit. Ceram. Soc.*, **51** 312 (1951-52).

34. F. Ya. Galakhov, "(III) System TiO_2-Al_2O_3-SiO_2," *Izvest. Akad. Nauk S.S.S.R., Otdel. Khim. Nauk*, 533 (1958).

35. G. V. Gibbs, L. W. Finger, and M. B. Boisen, Jr., "Molecular Mimicry of the Bond Length-Bond Strength Variations in Oxide Crystals," *Phys. Chem. Minerals*, **14** 327-31 (1987).

36. H. P. Kirchner, "Thermal Expansion Anisotropy Oxides and Oxide Solid Solutions," *J. Am. Ceram. Soc.*, **52** [7] 379-86 (1969).

37. M. Ishitsuka, T. Sato, T. Endo, and M. Shimada, "Synthesis and Thermal Stability of Aluminum Titanate Solid Solutions," *J. Am. Ceram. Soc.*, **70** [2] 69-71 (1987).

38. I. A. Aksay and J. A. Pask, "Stable and Metastable Equilibia in the System SiO_2-Al_2O_3," *J. Am. Ceram. Soc.*, **58** [11-12] 507-19 (1975).

39. R. M. Hazen and L. W. Finger, Comparative Crystal Chemistry: Temperature, Pressure, Composition, and the Variation of Crystal Structure, John Wiley & Sons, 1982.

40. P. Robinson and E. R. McCartney, "Subsolidus Relations in the System SiO_2-Al_2O_3-P_2O_5," *J. Am. Ceram. Soc.*, **47** [11] 590-98 (1964).

41. W. F. Horn, "The Studies of the Quaternary System B_2O_3-Al_2O_3-SiO_2-P_2O_5," Ph.D Thesis, Penn. State, 1974.

42. D. K. Agrawal and V. S. Stubican, "Germanium-Modified Cordierite Ceramics with Low Thermal Expansion," *J. Am. Ceram. Soc.*, **69** [12] 847-51 1986. br. 43. R. D.

Shannon, "Revised Effective Ionic Radii and Systematic Studies of Interatomic Distances in Halides and Chalcogenides," *Acta Cryst.*, A32 751-67 (1976).

44. Y. Nurishi and J. A. Pask, "Sintering of Al_2O_3-Amorphous Silica Compacts," *Ceram. Int.*, **8** [2] (1982)

45. C. W. Burnham, "The Crystal Structure of Mullite," *Carnegie Inst. Washington Yearbook.*, **62** 158-65 (1963).

46. H. Nakabayashi, K. Nishiwaki, and A. Ueno, "Characterization of A Binary Oxide Composed of SiO_2 and TiO_2," *Mat. Res. Bull.*, **23** 555-62 (1988).

47. H. D. Megaw, "Crystal Structure and Thermal Expansion," *Mat. Res. Bull.*, **6** 1007-18 (1971).

48. R. M. Hazen and C. T. Prewitt, "Effect of Temperature and Pressure on Interatomic Distances in Oxygen-Based Minerals," *Am. Mineral.*, **62** 309-15 (1977).

49. R. M. Rose, L. A. Shepard, and J. Wulff, The Structure and Properties of Materials, Vol. 4, Electronic Properties, John Wiley & Sons, Inc., 1966.

50. Y. S. Touloukian, R. K. Kirby, R. E. Taylor, and T. Y. R. Lee, Thermal Expansion, IFI/Plenum, New York, 1970.

51. D. Taylor, "The Thermal Expansion Behaviour of the Framework Silicates," *Mineral. Magazine*, **3** [38] 593-604 (1972).

51. J. K. Winter and S. Ghose, "Thermal Expansion and High-Temperature Crystal Chemistry of the Al_2SiO_5 polymorphs," *Am. Mineral.*, **64** 573-86 (1979).

Appendix 1

Reproducibility of CTE measurements on the automatic differential dilatometer

The sol-gel decomposed mullite powder from one batch was pressed into ten identical bar specimens which then were sintered at 1550°C for 72 hours. The results of the measurements are as follows:

Measurement No.	CTE($°C \times 10^6$) (R.T.—1000°C)
1	5.16
2	5.22
3	5.18
4	5.08
5	5.14
6	5.23
7	5.07
8	5.20
9	5.15
10	5.17

$$\mu = \frac{\sum_{i=1}^{10} CTE_i}{10} = 5.16 \times 10^{-6}/°C$$

$$\sigma = \left[\frac{\sum_{i=1}^{10} (CTE_i - \mu)^2}{10 - 1} \right]^{\frac{1}{2}} = 0.053 \times 10^{-6}/°C$$

$$\text{Coefficient of Variation} = \frac{\sigma}{\mu} = 1\%$$

Appendix 2

CTEs of Ga_2O_3-modified mullite measured on the automatic differential dilatometer

Sample No.	Composition (wt%)* x $(Al_{6-x}Ga_x)Si_2O_{13}$	Al_2O_3	SiO_2	Ga_2O_3	Phase	CTE($°C \times 10^7$) R.T.-1000°C
E0	0.00	71.79	28.21	0.00	M	53.0
E4	0.25	66.78	27.38	5.84	M	--
E6	0.50	62.67	26.86	10.47	M	51.4
E7	0.70	59.26	26.35	14.39	M	54.7
E8	0.90	55.97	25.87	18.16	M	54.6
E1	1.00	54.37	25.64	19.99	M	--
E10	1.20	51.26	25.18	23.56	M	--
E16	1.50	46.81	24.51	28.68	M	--
E42	1.60	45.36	24.30	30.34	M	53.1
E17	1.80	42.57	23.89	33.54	M	53.5
E18	2.00	39.86	23.50	36.64	M	54.0

* Samples were prepared by Erich Schwarz.

The vita has been removed from the scanned document